Extraction of Human Mandible Bones from Multi-Slice Computed Tomographic Data

Tamer M. Nassef
Computer and Programming Engineering Dept.
Misr University for Science and Technology, MUST
6th of October City, Egypt
tamer.nassef@k-space.org

Mohamed Alkhodary, Mona K. Marei
Tissue Engineering Lab.
Alexandria University
Alexandria, Egypt

Nahed H. Solouma
National Institute of Laser Science
Cairo University
Giza, Egypt

Yasser M. Kadah
Biomedical Engineering Dept.
Cairo University
Giza, Egypt

Abstract— **A new approach for segmenting different anatomical regions in dental Computed Tomography (CT) studies is presented in this paper. It is expected that the proposed approach will help automate different tissues regions by providing initial boundary points for deformable models or seed points for split and merge segmentation algorithms. Preliminary results obtained for dental CT studies of dentate and edentulous human-mandible are presented with finite element models divided by tetrahedral elements, which built based on actual CT data combined with triangulation equations. Identification of different anatomical regions set for mandible cortical and cancellous bones by generated 3D models by marching cubes technique.**

Keywords-medical imaging; tissue engineeing; 3D bone reconstruction; dental computed tomography

I. INTRODUCTION

Image scanners devices such as computed tomography (CT), magnetic resonance imaging (MRI) or positron emission tomography (PET) are nowadays a standard instrument for diagnosis. Among these devices, CT-scanners are today widely used at radiotherapy departments all over the world it have several advantages. The main advantages of a CT-scanner are to obtain physical information, like patient anatomy, size, shape, and in homogeneities; the other is to obtain the electron density from the different anatomical structures of the patient for the radiotherapy treatment planning [1]. Image segmentation is one of the primary steps in image analysis for object identification. The main aim is to recognize homogeneous regions within an image as distinct and belonging to different objects, where the segmentation process can be based on actual Digital Imaging and Communications in Medicine DICOM data to find the maximum homogeneity in grey levels within the regions identified.

A variety of techniques have been proposed for CT image segmentation methods. These methods can be classified into three categories. The first category includes analytic methods, in which segmentation algorithms are treated directly by considering some measure, which by a priori knowledge is assumed to be the appropriate measure, Tognola, et al has extracted the mandible contour by histogram equalization and thresholding and proposed another method by gradient vector flow snake parameters were optimized in order to achieve more accurate contours segmentation of nerve mandibular scans [2]-[4]. In 2009 Campadelli, et al applying hierarchical gray level based on framework to segment heart, bones, liver, kidneys, and spleen directly related to the Hounsfield units (HU) based on; gray level, learning and model fitting techniques with probabilistic atlases, and level set anatomical knowledge to obtained three dimensional (3D) binary image [5]. Typically this measure was incorporated into the original segmentation algorithm as well.

The second category includes supervised evaluation methods. In these methods, the results of a segmentation algorithm are compared to a "standard" reference image that is manually segmented beforehand, and the amount of discrepancy becomes the measure of segmentation effectiveness. Pileicikiene, et al choosing dead person for the study the precision of CT examination increased – voluntary and involuntary movements of research object were excluded (like breathing or muscle tonus movements), this make the segmentation more easier since the high resolution images captured by increasing the dose to get more than 1500 slice from the CT scanner [6]. Chen, et al has chosen the same condition with another method by comparing between dead and alive person. The author used commercial software to segment the DICOM images based on threshold and region growing methods to extract the mandible for a patient [7].

Liu, et al has used the same commercial software in his studies, but here the Temporomandibular Joint (TMJ) appear clearly in the 3D model geometry information of the cortical bones, cancellous bones and teeth are exported from commercial software; this may accomplished by semi-automated method [8]. This is the most commonly used method for medical segmentation. However, manually generating a reference image is a difficult, subjective, and time-consuming job, and generally cannot guarantee that one

978-1-4244-7000-6/11/$26.00 ©2011 IEEE

manually-generated segmentation image is better than another. Consequently, comparison using such reference images cannot ensure accurate evaluations.

The third category includes unsupervised evaluation. In these methods, the segmentation results are evaluated by judging the quality of the segmented image directly to evaluate some pre-defined criteria, such as the partitioning of foreground objects from the background, Reina, et al present a 3D surface model of mandible based on morphological analysis with standard distances without case study and this near to the information theory. Since the shape of each organ is not consistent throughout all slices of a 3D medical image and the gray level intensities overlap considerably for soft tissues, texture is especially important in medical image segmentation because of its homogeneity within the same tissue and across different slices. Once textures have been calculated and their scalar values assigned to pixels, the pixels can be clustered or classified (when the tissues' labels are available) for the purpose of segmentation [9]. These evaluation measures are typically used with gray-level images and are not designed for general-purpose applications.

The use of numerical methods such as finite element methods (FEM) has been adopted in solving complicated geometric problems, as it is very difficult to achieve an analytical solution. FEM is a technique for obtaining a solution to complex mechanical problems by dividing the domain problem into a collection of much smaller and simpler domains (elements) where field variables can be interpolated using shape functions [12]. In 1977, Weinstein was the first to use FEM in implant dentistry. Subsequently [10], FEM was rapidly applied in many aspects of implant dentistry. Atmaram and Mohammed analyzed the stress distribution in a single tooth implant, to understand the effect of elastic parameters and geometry of the implant, implant length variation, and pseudo-periodontal ligament incorporation [11]-[13]. Borchers and Reichart performed a three-dimensional (3D) FEM of an implant at different stages of bone interface development [14]. Cook, et al. applied it in porous rooted dental implants [15]. Meroueh, et al. used it for an osseointegrated cylindrical implant [16]. Williams, et al. carried it out on cantilevered prostheses on dental implants [17]. Akpinar, et al. simulated the combination of a natural tooth with an implant using FEM [18].

In the present study, a new approach for segmentation based on actual CT data are used to extract an accurate human mandible with TMJ and teeth to help for generating robust 3D surfaces and volumetric models. The proposed technique used the statistical texture method applying triangulation equations combined with information captured from HU based on gray-level techniques, finally marching cubes technique are used to build the prototype geometry for the full-human mandible.

II. Materials and Methods

Dentate and edentulous patient's mandible was scanned with SIEMENS/Esprit CT machine 120 KV energy. The pixel size of the scanner is 512x512 pixels, and 0.4 mm is equal to the distance between CT slice planes. Totally 400 images were obtained raw data was in Digital Imaging and Communications in Medicine (DICOM) format. The electron density is obtained from the CT-scanner through Hounsfield units (HU) as in (1), DICOM carries all information about CT scanner, Table I presence some of useful information.

$$HU = 1000\left(\frac{\mu - \mu_{water}}{\mu_{water}}\right). \quad (1)$$

Here μ is the linear attenuation coefficient for the respective material. Campadelli, et al has segmented different tissues based on HU range from CT, each slice has different HU range and this helps in applying the threshold technique to eliminate the undesired tissues and focus on the mandible regions only. Noise produced by the reflection rays from filling materials, it cannot appear clearly in axial planes, but it evidently become visible at the 3D model as shown in Fig. 1., where The 3D model and panoramic image are captured from the CT scanner directly without any enhanced or segmented procedures [5]. Tognola, et al has proposed a segmentation technique to reduce the noises caused by "star-shaped" artifacts, due to dental or mandible metallic implants, this technique based on the threshold method [3]. New technique is produced to reduce all noises from the DICOM raw data without any conversions of formats to keep DICOM information based on the same theory at [3] and [5], which used to separate all the mandible regions and build robust 3D models, where the mandible regions can be separated to multi-objects (i.e. teeth, TMJ, body …etc). Proposed segmentation technique is used to extract these regions from the CT slices based on triangulation theory as in (2) and (3) as described at Fig. 2. [19], which is implemented with MATLAB program. Triangulation process method is used to generate the 2.5D models and the marching cubes are used for generating the final 3D model; the output triangle mesh of the mandible must define a closed 2-manifold in order to represent a volume and allow for 3D-meshing. This implies that no vertex of the triangle mesh is complex and each edge of the triangle mesh belongs to exactly two triangles.

$$\frac{x_{slice}-x_{pixel}}{f} + \frac{m_{11}(x_j-x_s)+m_{12}(y_j-y_s)+m_{13}(z_j-z_s)}{m_{31}(x_j-x_s)+m_{32}(y_j-y_s)+m_{33}(z_j-z_s)} = 0. \quad (2)$$

$$\frac{y_{slice}-y_{pixel}}{f} + \frac{m_{21}(x_j-x_s)+m_{22}(y_j-y_s)+m_{23}(z_j-z_s)}{m_{31}(x_j-x_s)+m_{32}(y_j-y_s)+m_{33}(z_j-z_s)} = 0. \quad (3)$$

Where

$$m_{11} = \cos\emptyset\cos\kappa$$
$$m_{12} = \cos\omega\sin\kappa + \sin\omega\sin\emptyset\cos\kappa$$

$$m_{13} = \sin\omega\sin\kappa - \cos\omega\sin\emptyset\cos\kappa$$

$$m_{21} = -\cos\emptyset\cos\kappa$$
$$m_{22} = \cos\omega\cos\kappa - \sin\omega\sin\emptyset\sin\kappa$$

$$m_{23} = \sin\omega\cos\kappa + \cos\omega\sin\emptyset\sin\kappa$$

$$m_{31} = \sin\emptyset$$
$$m_{32} = -\sin\omega\cos\emptyset$$

$$m_{33} = \cos\omega\cos\emptyset$$

TABLE I. INFORMATION SAMPLES CARRIED BY DICOM FILES

Rows	512	Columns	512
Rescale Intercept	-1024	Rescale Slope	1
KVP	120	Reconstruction Diameter	200
Exposure Time	2000	X-ray Tube Current	45

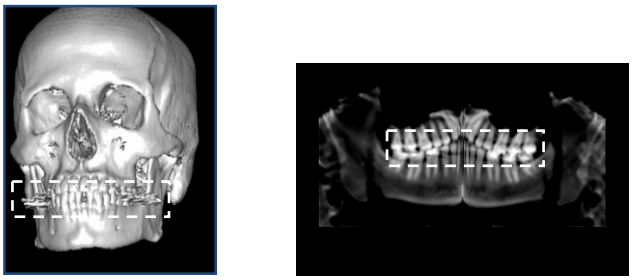

a b

Figure 1. Filling materials noises; (a) 3D model for a mandible as a part of a skull, (b) panoramic x-ray, the Wight dashed rectangles refers to the filling cavity material that cause the noise.

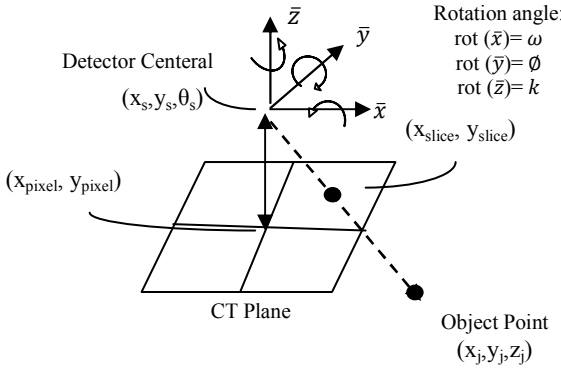

Figure 2. Nomenclature for the triangulation equations.

In its original version the Marching Cubes algorithm only produces a set of triangles without neighborhood information and it does not take care of this special topological requirements, where the output triangle set contains complex vertices as well as edges that share more than two triangles. Such cases occur if one or more intersection points between the edges of a cube and the object are equal to a vertex P_{ijk} of the cube. In this cases triangles as they are stored in the look-up tables of the marching cubes algorithm degenerate to edges or vertices.

III. RESULTS

Three different models are provided from this approach, Fig. 3 represents models for the dentate patient, who used to validate the technique by comparing between the provided model from phantom software at the CT scanner and the proposed model, full skull with and without skin are shown as different objects. Table II shows the comparison between Multi-object models with DICOM images and phantom software at the CT scanner, where the TMJ that hides behind the skull bone appears with Multi-object models, the artifacts noise from felling metals or implants and undesired soft tissues has been reduced.

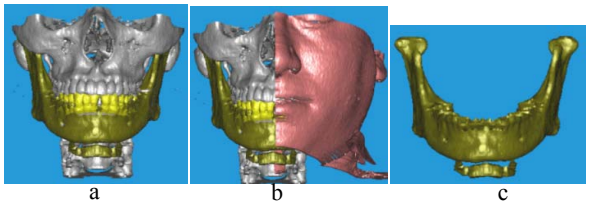

a b c

Figure 3. Multi-objects 3D model; (a) all objects with skin section, (b) full skull without skin, (c) full mandible with Hyoid bone and TMJ.

TABLE II. VALIDATION OF OUTPUT MODELS

Category	*Phantom Software*	*DICOM*	*Multi-object Model*
Artifacts noise	✓	✓	null
Soft tissue interference	12% to 20%	null	2%
TMJ	null	✓	✓

For edentulous patients Fig. 4 represents models for two types of mandible bone, where the trabiculer pattern is evaluated for the cancellous bone, which can be exported to finite element program with STL format. Abacus program are used to provide a finite element model for the trabicular pattern meshed with second order tetrahedrons (Tet10), which have ten nodes (four corner and additional six edge nodes) and produce more accurate analysis results than first order tetras as shown in Fig. 5 with implant loading.

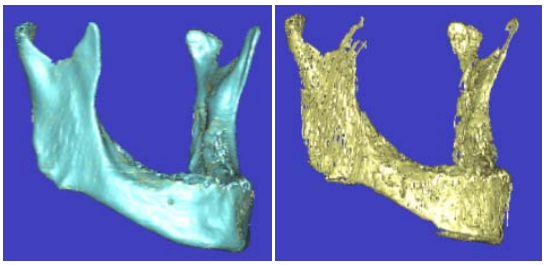

a b

Figure 4. Mandible 3D bones model with TMJ; (a) Cortical bone, (b) Cancellous bone.

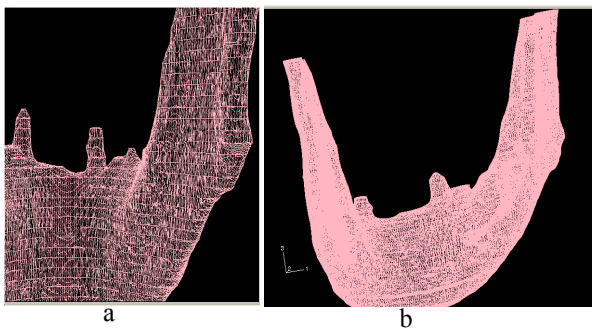

a b

Figure 5. Mandible FEM, Meshing mandible model after loading implant; (a) Cortical bone, (b) Both cortical and cancellous bone.

IV. DISCUSSION

Steven, et al [20] has stated that the resolution of CT images is not as good as that obtained from micro-imaging techniques; however, it is sufficient to visualize the trabecular network. Using the earlier developed automated meshing techniques (voxel conversion technique providing meshes with brick elements and the marching cube algorithm providing meshes with tetrahedral elements); such images provided a basis for the generation of finite element models that represent the trabecular morphology of entire bones in human mandible. These models allowed non-destructive assessment of mechanical properties of bone at resolutions that were not previously possible. A computer program was written in MATLAB code for implementing the segmentation process applied on all DICOM planes; all planes are assembled with 'OpenGl algorithms'. Multi-objects regions enveloped with texture material to verify their prosperities. Textured models are created by evaluating the vertex (x, y, z) of model from origin (0, 0, 0) pixels positions can be calculated. FE model are generated after idealization the geometry and meshed with second order tetrahedrons, which each element has mathematical relations that describe how degrees of freedom of one node relate to the next.

V. CONCLUSION

The multi-object reconstruction helps in finite element analysis (FEA); that the FE models will have specific information about organs; this helps in reducing the time of solving the mechanical problems. Many investigators have evaluated 3D models from CT 2D images. The results of these studies have been approximated for the conversion of images formats, this study provide a realistic 3D mandible model with TMJ from 2D segmented images scanned with CT scanner device based on actual CT data carried by DICOM files formats, where TMJ and "coronoid process" regions separation processes were difficult since their positions at the back of the face bone, these models can helps in dental diagnosing and to evaluate the orthogonal mechanical properties values especially for edentulous patients. The noises produced for filling cavity materials or dental implants are eliminated by combined classical segmentation techniques. Tetrahedral elements are suitable to divide the mandible model to finite elements for mechanical analysis studies like implant stress-strain; multi-objects technique separate mandible to objects for decreasing the number of nodes and elements to reduce the number of FEA equations; this will accelerate the idealization process at FEM models.

REFERENCES

[1] H.Y. Shum, S.C. Chan, and S.B. Kang, "Image-Based Rendering," Springer Science-Business Media, LLC, Spring Street, New York, USA, 2007.

[2] G. Tognola, M. Parazzini, G. Pedretti, P. Ravazzani, F. Grandori, A. Pesatori, M. Norgia, and C. Svelto, "Optimization of 2D to-3D Reconstruction Technique for Maxillofacial Surgery Applications," IEEE / IST International Workshop on Imaging Systems and Techniques - Italy, pp.186-189, April 2006.

[3] G. Tognola, M. Parazzini, G. Pedretti, P. Ravazzani, and C. Svelto, "Three-Dimensional Reconstruction and Image Processing in Mandibular Distraction Planning," IEEE Trans. instrumentation and measurement, vol. 55, pp.1959-1964, December 2006.

[4] G. Tognola, M. Parazzini, G. Pedretti, P. Ravazzani, F. Grandori, A. Pesatori, M. Norgia, and C. Svelto, "Novel 3D reconstruction method for mandibular distraction planning," Proceedings of IST - IEEE, Italy, pp.82-85, April 2006.

[5] P. Campadelli, E. Casiraghi, S. Pratissoli, and G. Lombardi, "Automatic Abdominal Organ Segmentation From CT Images," Electronic Letters on Computer Vision and Image Analysis, vol. 8, pp.1-14, 2009.

[6] G. Pileicikiene, E. Varpiotas, R. Surna, and A. Surna, "A Three-Dimensional Model of the Human Masticatory System, Including the Mandible, the Dentition and the Temporomandibular Joints," J. Baltic Dental and Maxillofacial, vol. 9 , pp. 27-32, 2007.

[7] M. Chen , L. Ni , Yu Zhang , Yuan Zhang "Comparison Study on the 3D Reconstruction of Mandible According to Virtul Chinese Human Slice Data and CT Data," J. Modelling and Simulation, vol. 3 , pp.235-240, 2007.

[8] Z. Liu, Y. Fan, and Y. Qian, "Biomechanical simulation of the interaction in the Temporo-mandibular Joint within dentate mandible: A Finite Element Analysis," Proceedings of ICME - IEEE, China, vol. 27, pp.1842-1846, 2007.

[9] J.M. Reina, J.M. García-Aznar, J. Domínguez, and M. Doblaré, "Numerical Estimation of Bone Density and Elastic Constants Distribution in a Human Mandible," J. Biomechanics, vol. 40, pp.828-836, 2007.

[10] A.M. Weinstein, J.J. Klawitter, S.C. Anand, and R. Schuessler, "Stress Analysis of Porous Rooted Dental Implants," J. Dental Res., vol. 55, pp.772-777, 1976.

[11] G.H. Atmaram, and H. Mohammed, "Stress Analysis of Single-Tooth Implants. I. Effect of Elastic Parameters and Geometry of Implant," Artificial Cells, Blood Substitutes and Biotechnology, vol. 7, pp.99-104, 1979.

[12] G.H. Atmaram, and H. Mohammed, "Stress Analysis of Single-Tooth Implants II. Effect of Implant Root-Length Variation and Pseudo Periodontal Ligament Incorporation," Artificial Cells, Blood Substitutes and Biotechnology, vol. 7, pp.105-110, 1979.

[13] H. Mohammed, G.H. Atmaram, and F.J. Schoen, "Dental implant design: a critical review," J. Oral Implantol., vol. 8, pp.393-410, 1979.

[14] L. Borchers, and P. Reichart, "Three-Dimensional Stress Distribution around a Dental Implant at Different Stages of Interface Development,"J. Dental Res., vol. 62, pp.155-159, 1983.

[15] S.D. Cook, A.M. Weinstein, and J.J. Klawitter, "A Three-Dimensional Finite Element Analysis of a Porous Rooted Co-Cr-Mo Alloy Dental Implant,"J. Dental Res., vol. 61, pp. 125-129, 1982.

[16] K.A. Meroueh, F. Watanabe, and P.J. Mentag, "Finite Element Analysis of Partially Edentulous Mandible Rehabilitated with an Osteointegrated Cylindrical Implant," J. Oral Implantol., vol. 13, pp. 215-238, 1987.

[17] K.R. Williams, C.J. Watson, W.M. Murphy, J. Scott, M. Gregory, and D. Sinobad, "Finite Element Analysis of Fixed Prostheses Attached to Osseointegrated Implants," in Quintessence Int., vol. 21, pp.563-570, 1990.

[18] I. Akpinar, F. Demirel, L. Parnas, and S. Sahin, "A Comparison of Stress and Strain Distribution Characteristics of two Different Rigid Implant Designs for Distal Extension Fixed Prostheses," in Quintessence Int., vol. 27, pp. 11-17, 1996.

[19] C. C. Slama, "Manual of Photogrammetry, " 4th ed. Bethesda, MD: Amer. Soc. Photogrammetry, Remote Sensing, 1980.

[20] K. Steven, b. Boyda, and M. Ralph, "Smooth surface meshing for automated finite element model generation from 3D image data," J. Biomechanics, vol. 39, pp. 1287–1295, 2006.